activity of Pd_2Cl_2(dpmMe)(dpm) (4), containing a single methyl group, toward CO can be rationalized similarly.

We note also that Pd_2Cl_2(dpmMe)(dpm) reacts with H_2S to form the bridged sulfide complex and molecular H_2,[38] exactly analogous to the $Pd_2Cl_2(dpm)_2$ system;[39] however, as with CO, the $Pd_2Cl_2(dpmMe)_2$ complex is unreactive toward H_2S.

Conclusions

An improved synthetic procedure for 1,1-bis(diphenylphosphino)ethane (dpmMe) has been found, and some mono- and dinuclear palladium complexes of this ligand have been synthesized and characterized, as well as dinuclear species with mixed-ligand systems (dpm or Ph_2Ppy). Structures of $PdCl_2$(dpmMe) (two independent molecules within the crystal lattice) are compared to those reported previously for the dpm, dpe, and dpp analogues; variations in Pd–P bond lengths correlate with displacement of the P atoms from the $PdCl_2$ plane and not, as suggested earlier, with steric constraints associated with the cis-bidentate ligands. The anti form of $Pd_2Cl_2(dpmMe)_2$ shows no reactivity in solution toward CO probably because an A-frame, bridged-carbonyl product would experience a steric problem associated with the presence of one of the methyl groups. The Pd_2Cl_2(dpmMe)(dpm) complex does bind CO reversibly, but with lower overall affinity than $Pd_2Cl_2(dpm)_2$; the data suggest that the mixed-ligand species, modified by attachment to a support through the methyl substituent, should bind CO reversibly.

Acknowledgment. We thank the U.S. Department of Energy, Morgantown Energy Technology Center, and the Natural Sciences and Engineering Research Council of Canada for financial support and Johnson Matthey Ltd. for loan of the palladium. We are grateful also to one reviewer who provided helpful comments regarding the CO reactivity pattern.

Supplementary Material Available: Figures 1, 3, and 7 (^1H NMR spectra of 1, 2, and 5) and tables of bond lengths, bond angles, torsion angles, hydrogen coordinates, and anisotropic thermal parameters for 1 and 2 and C–H···Cl interactions for 1 (21 pages); listings of structure factors for 1 and 2 (64 pages). Ordering information is given on any current masthead page.

---

[38] Besenyei, G.; Lee, C. L.; James, B. R.; Nelson, D. A.; Lilga, M. A., to be submitted for publication.

[39] Lee, C. L.; Besenyei, G.; James, B. R.; Nelson, D. A.; Lilga, M. A. *J. Chem. Soc., Chem. Commun.* **1985**, 1175.

Addition of the Os–CH_2 Bond in $Os_3(CO)_{11}(\mu\text{-}CH_2)$ to $Pt(PPh_3)_2$ To Give the Spiked Triangular Cluster $Os_3Pt(\mu\text{-}CH_2)(CO)_{11}(PPh_3)_2$. An NMR Investigation of the Fluxional Properties of $Os_3(CO)_{11}(\mu\text{-}CH_2)$

Gregory D. Williams, Marie-Chantal Lieszkovszky, Chad A. Mirkin, and Gregory L. Geoffroy*

Department of Chemistry, The Pennsylvania State University, University Park, Pennsylvania 16802

Arnold L. Rheingold

Department of Chemistry, University of Delaware, Newark, Delaware 19716

Received February 19, 1986

$Os_3(CO)_{11}(\mu\text{-}CH_2)$ (1) reacts with $(Ph_3P)_2Pt(C_2H_2)$ to give the new tetranuclear cluster $Os_3Pt(\mu\text{-}CH_2)(CO)_{11}(PPh_3)_2$ (2) in which the methylene ligand bridges an Os–Pt bond. Compound 2 has been characterized spectroscopically and by an X-ray diffraction study. It crystallizes in the space group $C2/c$ with $a = 39.18$ (2) Å, $b = 15.200$ (6) Å, $c = 18.532$ (7) Å, $\beta = 91.17$ (3)°, $V = 11034$ (8) Å^3, and $Z = 8$. The structure has been refined for the 3258 reflections with $F_o > 5\sigma(F_o)$ to R and R_{wF} values of 0.0557 and 0.0624. The cluster has a "spiked triangular" geometry with the Pt atom bonded to only one Os of the Os_3 triangle. The methylene ligand bridges the Os–Pt bond, and the Pt is further coordinated by two PPh_3 ligands. Compound 2 readily and reversibly exchanges CO for PPh_3 at the Pt center. Magnetization-transfer experiments (^1H, ^{13}C) have shown that the inequivalent methylene hydrogens in the parent cluster 1 undergo slow exchange, but the spectral evidence does not imply the intermediacy of a terminal Os=CH_2, in contrast to the recently reported fluxional properties of $Ru_3(CO)_{11}(\mu\text{-}CH_2)$.

The methylene-bridged cluster $Os_3(CO)_{11}(\mu\text{-}CH_2)$ (1)[1] has proven to be unusually reactive. Even though it is coordinatively saturated, it readily reacts with CO,[2a] SO_2,[2b] $SnCl_2$,[2c] N_3^-, NO_2^-, Cl^-, Br^-, and I^-[2d] under mild conditions to give a variety of new products. We have been interested

---

[1] (a) Steinmetz, G. R.; Morrison, E. D.; Geoffroy, G. L. *J. Am. Chem. Soc.* **1984**, *106*, 2559–2564. (b) Shapley, J. R.; Sievert, A. C.; Churchill, M. R.; Wasserman, H. J. *J. Am. Chem. Soc.* **1981**, *103*, 6975–6977. (c) Johnson, B. F. G.; Lewis, J.; Raithby, P. R.; Sankey, S. W. *J. Organomet. Chem.* **1982**, *231*, C65–C67. (d) Arce, A. J.; Deeming, A. J. *J. Chem. Soc., Chem. Commun.* **1982**, 364–365.

[2] (a) Morrison, E. D.; Steinmetz, G. R.; Geoffroy, G. L.; Fultz, W. C.; Rheingold, A. L. *J. Am. Chem. Soc.* **1984**, *106*, 4783–4789. (b) Morrison, E. D. Ph.D. Thesis, The Pennsylvania State University, 1985. (c) Viswanathan, N.; Morrison, E. D.; Geoffroy, G. L.; Gieb, S. J.; Rheingold, A. L., *Inorg. Chem.*, submitted for publication. (d) Morrison, E. D.; Geoffroy, G. L.; Rheingold, A. L.; Fultz, W. C. *Organometallics* **1985**, *4*, 1413–1418.

0276-7333/86/2305-2228$01.50/0 © 1986 American Chemical Society

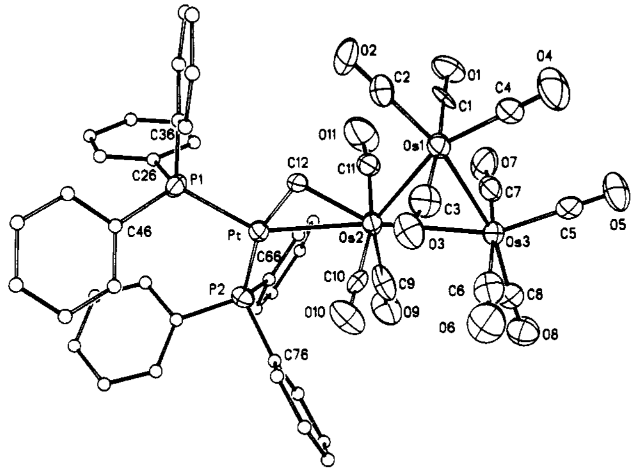

Figure 1. Molecular structure and labeling scheme for $Os_3Pt(CO)_{11}(\mu\text{-}CH_2)(PPh_3)_2$ (2).

in the synthesis and chemistry of μ-CH_2 clusters with four or more metal atoms and accordingly considered the preparation of tetrametallic $MOs_3(\mu\text{-}CH_2)$ clusters by the addition of appropriate metal fragments to 1. Herein we describe the high-yield synthesis of the spiked triangular $PtOs_3$ cluster 2 by such a reaction with $Pt(PPh_3)_2(CH_2{=}CH_2)$ (eq 1) and its characterization by an X-ray diffraction study.

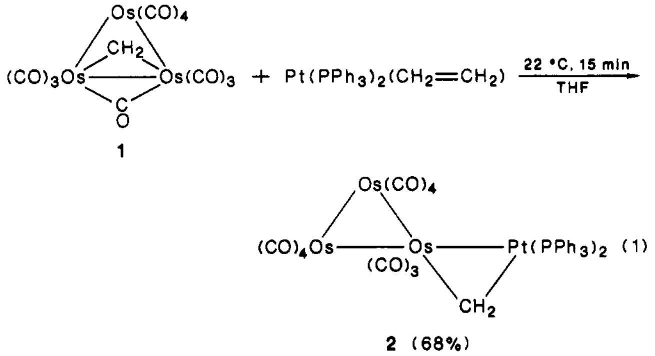

Consideration has been given to the mechanism of formation of 2, and particularly interesting is the possibility of addition of "$Pt(PPh_3)_2$" across an $Os{=}CH_2$ linkage in an activated form of 1. Although the methylene ligand in 1 bridges two Os atoms in its ground-state structure, a terminal methylene complex may be energetically accessible. Indeed, a recent study of the Ru analogue of 1, $Ru_3(CO)_{11}(\mu\text{-}CH_2)$, showed that the intermediacy of a terminal methylene complex best accounts for its fluxional properties.[3] We accordingly examined by NMR spectroscopy the fluxional properties of 1, and we show herein that they are different from those of its Ru analogue with no evidence obtained for a terminal methylene intermediate.

Results and Discussion

Synthesis of $Os_3Pt(\mu\text{-}CH_2)(CO)_{11}(PPh_3)_2$ (2). The reaction of $Os_3(CO)_{11}(\mu\text{-}CH_2)$ with $(Ph_3P)_2Pt(C_2H_4)$ proceeds smoothly at room temperature to give 2 in good yield (eq 1). Infrared monitoring of the reaction showed no detectable intermediates and only disappearance of the starting complexes. Complex 2 has been characterized spectroscopically and by an X-ray diffraction study (Figure 1). Its spectroscopic data summarized in the Experimental Section are consistent with the determined structure, except that the ^1H NMR spectrum shows that the μ-CH_2 protons couple with only one of the phosphorus atoms, presumably the one in a trans location. Likewise, the ^{13}C NMR spectrum of 2 shows coupling of the methylene carbon to only one phosphorus atom. Complex 2 is moderately air-sensitive in solution, decomposing within ~15 min of air exposure, although it can easily be handled as a solid in air without noticeable decomposition.

Table I. Selected Bond Distances and Angles for $Os_3Pt(CO)_{11}(\mu\text{-}CH_2)(PPh_3)_2$

Bond Distances (Å)			
Os(1)-Os(2)	2.877 (4)	Os(2)-Pt	2.772 (4)
Os(1)-Os(3)	2.857 (3)	Pt-P(1)	2.25 (1)
Os(2)-Os(3)	2.882 (4)	Pt-P(2)	2.33 (1)
Os(2)-C(12)	2.02 (4)	Pt-C(12)	1.95 (6)
Bond Angles (deg)			
Os(1)-Os(2)-Os(3)	59.5 (1)	Os(1)-Os(2)-Pt	132.3 (1)
Os(2)-Os(3)-Os(1)	60.2 (1)	Os(3)-Os(2)-Pt	168.2 (1)
Os(3)-Os(1)-Os(2)	60.3 (1)	Pt-C(12)-Os(2)	89 (2)
P(1)-Pt-P(2)	105.5 (6)	Os(2)-Pt-C(12)	47 (1)
P(1)-Pt-Os(2)	141.4 (4)	Pt-Os(2)-C(12)	45 (1)
P(2)-Pt-Os(2)	112.5 (4)		

Structural Characterization of 2. The molecular structure of 2 is shown in Figure 1 with relevant bond distances and angles listed in Table I. The molecule consists of a triangle of Os atoms, two of which are ligated by four CO ligands and the third, Os(2), by three CO ligands. The Pt atom is ligated by two PPh_3 ligands and also by the μ-CH_2 ligand which bridges the Os(2)-Pt bond. The coordination geometry about Pt is best described as a distorted square plane with the maximum deviation from the P(1)-P(2)-Pt-C(12)-Os(2) least-squares plane of 0.108 Å associated with C(12). The Pt coordination is also reminiscent of the trigonal-planar geometry found in $(PPh_3)_2Pt(CH_2{=}CH_2)$[4] and an interesting description of 2 is with an $Os{=}CH_2$ linkage π-bonded to Pt.

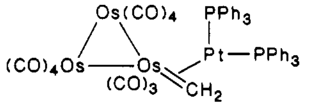

The Os-Pt bond length of 2.772 (4) Å falls within the 2.717-3.015 Å range observed for other Os_3Pt clusters,[5] and the Os-Os distances compare well to the typical Os-Os single bond distance of 2.877 (3) Å found in $Os_3(CO)_{12}$.[6]

To our knowledge, no other examples of methylene ligands bridging Os-Pt bonds have been reported. However, a bond length comparison can be made to other compounds which contain Os-CH_2 and Pt-CH_2 bonds. The Os-C(12) distance of 2.02 (4) Å in 2 is ~0.1 Å less than the 2.125 (7) -2.15 (1) Å range found for Os-C(methylene) bonds in other $Os_x(\mu\text{-}CH_2)$ clusters.[5b,7] The Pt-CH_2 bond length of 1.95 (6) Å in 2 is within statistical error of the 2.01 (2) Å Pt-C distance in $Pt_2Cl_2(\mu\text{-}CH_2)(\mu\text{-}dppm)_2$ and only slightly shorter than the Pt-C distance of 2.13 (3) Å in $[Pt_2Cl(CH_2PPh_3)(\mu\text{-}CH_2)(\mu\text{-}dppm)_2][PF_6]$.[8]

---

(3) Holmgren, J. S.; Shapley, J. R. *Organometallics* **1985**, *4*, 793–794.

(4) (a) Cheng, P.-T.; Cook, C. D.; Nyburg, S. C.; Wan, K. Y. *Inorg. Chem.* **1971**, *10*, 2210–2213. (b) Cheng, P.-T.; Nyburg, S. C. *Can. J. Chem.* **1972**, *50*, 912–916.

(5) (a) Farrugia, L. J.; Howard, J. A. K.; Mitrprachachon, P.; Stone, F. G. A.; Woodward, P. *J. Chem. Soc., Dalton Trans.* **1981**, 162–170. (b) Farrugia, L. J.; Green, M.; Hankey, D. R.; Murray, M.; Orpen, A. G.; Stone, F. G. A. *J. Chem. Soc., Dalton Trans.* **1985**, 177–190.

(6) Churchill, M. R.; DeBoer, B. G. *Inorg. Chem.* **1977**, *16*, 878–884.

(7) Calvert, R. B.; Shapley J. R.; Schultz, A. J.; Williams, J. M.; Suib, S. L.; Stucky, G. D. *J. Am. Chem. Soc.* **1978**, *100*, 6240–6241.

(8) Azam, K. A.; Frew, A. A.; Lloyd, B. R.; Manojlovic-Muir, L.; Muir, K. W.; Puddephatt, R. J. *Organometallicsw* **1985**, *4*, 1400–1406.

Scheme I

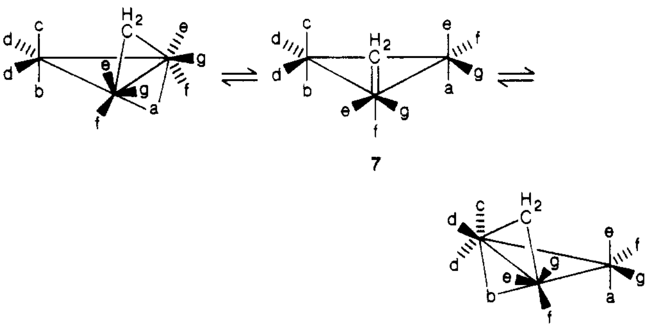

7

The structure of **2** is markedly different from the structures of the other two reported $Os_3Pt(\mu\text{-}CH_2)$ clusters which were prepared by Stone and co-workers[5b] from addition of CH_2N_2 to $Os_3Pt(CO)_{10}(\mu\text{-}H)_2P(C_6H_{11})_3$. These are isomers of $Os_3Pt(CO)_9(\mu\text{-}H)_2(\mu\text{-}CH_2)P(C_6H_{11})_3$ and have the structures depicted in **3** and **4** with tetrahedral metal frameworks and with the methylene ligands bridging Os–Os bonds. In contrast, cluster **2** has the spiked triangular geometry shown in Figure 1. We attempted to convert **2** into a compound with a structure similar to **3** or **4** by heating to expel CO and close the metal framework but were unsuccessful.

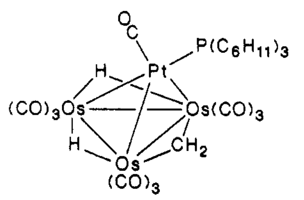

3

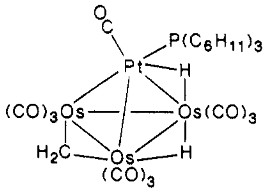

4

Reaction of 2 with CO. The methylene cluster **1** reacts with CO to give a new cluster containing the $\mu\text{-}CH_2CO$ ketene ligand.[2a] We anticipated a similar reaction with cluster **2** but instead observed rapid substitution of a CO lignd for PPh_3 to give complex **5** (eq 2). Complex **5** is stable in solution when kept under a CO atmosphere, but removal of the CO from above the solution induces slow (~2–4 h) reformation of **2**. Also, all attempts to isolate pure **5** by crystallization or by chromatography gave instead complex **2**. Complex **5** was thus spectroscopically characterized in solutions kept under CO. Its ^{13}C NMR spectrum showed a triplet for the $\mu\text{-}CH_2$ ligand at δ 73.1 with $J_{^{13}C-^{1}H}$ = 146 Hz, but no $^{13}C-^{31}P$ coupling was observed. Recall that the methylene ^{13}C NMR resonance of complex **2** showed coupling to only one of the phosphorus atoms, and it is presumably this trans phosphorus which has been replaced by CO. The ^1H NMR spectrum of **5** shows a multiplet at δ 4.30 due to the $\mu\text{-}CH_2$ ligand. At −80 °C, the ^{31}P NMR spectrum of **5** shows two sharp resonances at δ 20.8 ($Pt\text{-}\mathit{P}Ph_3$, $J_{^{31}P-^{195}Pt}$ = 4088 Hz) and −6.6 (free $\mathit{P}Ph_3$). Upon warming to room temperature, these resonances broaden considerably, indicating that rapid exchange of free and complexed PPh_3 occurs.

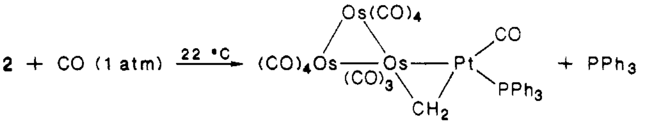

5

(2)

Infrared spectral changes indicate that complex **2** reacts with PhC≡CPh in a manner similar to that observed with CO, with the alkyne replacing one of the PPh_3 ligands. However, these reactions were not further studied.

Fluxional Properties of $Os_3(CO)_{11}(\mu\text{-}CH_2)$ (1) and Its Relevance to the Mechanism of Formation of 2. The $\mu\text{-}CH_2$ cluster **1** has proven to be unusually reactive for a coordinatively saturated cluster as evidenced by its facile reactions with CO,[2a] SO_2,[2b] halides,[2d] and $SnCl_2$[2c] and as described herein with "$Pt(PPh_3)_2$", formed in situ from $(CH_2{=}CH_2)Pt(PPh_3)_2$. Mechanistic studies of the reaction of **1** with CO indicates that this reaction may proceed via the intermediacy of a coordinatively unsaturated ketene cluster, **6**, formed by insertion of one of the initial cluster CO's into an Os–CH_2 bond (eq 3).[2a] The high reactivity of **1** with CO, halides, SO_2, and $SnCl_2$ can be rationalized by addiiton of these reagents to the open coordination site in **6**, followed by deinsertion of CO from the ketene ligand and subsequent CO loss if necessary.

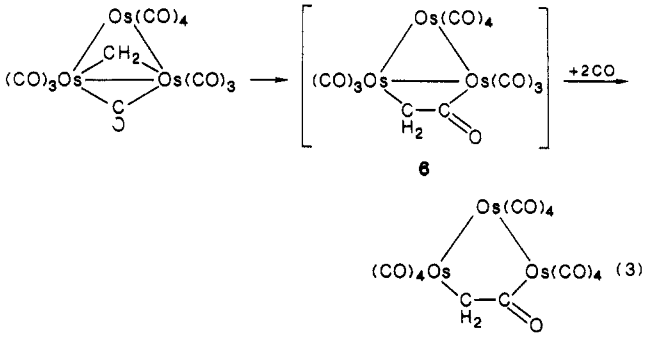

(3)

The reaction of $(CH_2{=}CH_2)Pt(PPh_3)_2$ with **1** could be explained by a similar process, but the structure of the product **2** suggests the alternative possibility of addition of PtL_2 across an $Os{=}CH_2$ bond of an intermediate Os_3 cluster with a terminal methylene ligand. Note that such reaction represents formal replacement of a $CH_2{=}CH_2$ ligand from the Pt coordination sphere by an $Os{=}CH_2$ ligand.

Such a suggestion is supported by Shapley and coworkers recent study of the fluxionality of the analogous cluster $Ru_3(CO)_{11}(\mu\text{-}CH_2)$ in which evidence was provided for the intermediacy of isomer **7** with a terminal $Ru{=}CH_2$ ligand (Scheme I).[3] The process illustrated in Scheme I explains the observed averaging of the methylene protons which are inequivalent in the static structure of $Ru_3(CO)_{11}(\mu\text{-}CH_2)$ as well as the ^{13}C NMR averaging of the μ-CO ligand with one of the axial carbonyls on the back Ru atom.

As previously reported,[1] the ^1H NMR spectrum of **1** at room temperature clearly shows the presence of inequivalent hydrogens with no evidence for an exchange process. The facile thermal transformation of **1** into $H_2Os_3(CO)_9(\mu_3\text{-}CCO)$[9] prohibits heating the sample to directly probe for an exchange process by standard NMR line-shape analysis. However, a ^1H NMR spin-magnetization-transfer experiment clearly showed that the inequivalent methylene protons do undergo slow exchange. Selective irradiation of the δ 7.75 doublet due to one of these methylene hydrogens caused a decrease in intensity of the δ 6.47 doublet due to the other, and a rate of 0.8 ± 0.4 s^{-1} can be estimated for this process.[10] Note that the rate of exchange of these hydrogens is substantially slower than that determined for $Ru_3(CO)_{11}(\mu\text{-}CH_2)$ (4.0 s^{-1} at 17 °C[3]).

The above data do not provide information as to the exact details of the exchange process in **1**. More infor-

---

(9) Sievert, A. C.; Strickland, D. S.; Shapley, J. R.; Steinmetz, G. R.; Geoffroy, G. L. *Organometallics* **1982**, *1*, 214–215.

(10) (a) Faller, J. W. *Determ. Org. Struct. Phys. Methods* **1973**, *5*, 75–97. (b) Anet, F. A. L.; Bourn, A. J. R. *J. Am. Chem. Soc.* **1967**, *89*, 760–768. (c) A plot of the kinetic data obtained from the ^1H NMR magnetization transfer experiment is available as supplementary material.

Table II. Crystal, Data Collection, and Refinement Parameters for $Os_3Pt(CO)_{11}(\mu\text{-}CH_2)(PPh_3)_2$ (2)

formula	$Os_3PtC_{48}H_{32}O_{11}P_2$	β, deg	91.15 (4)
fw	1612.3	V, Å^3	11032 (9)
cryst system	monoclinic	Z	8
space group	$C2/c$	ρ(calcd) g/cm^3	1.941
a, Å	39.15 (2)	μ, cm^{-1} (Mo $\kappa\alpha$)	96.61
b, Å	15.202 (8)	T, °C	23
c, Å	18.542 (8)		
diffractometer	Nicolet R3	scan speed, deg min^{-1}	6
radiatn	Mo $\kappa\alpha$ (λ = 0.71073)		
monochromator	graphite	rflns collected	5425
scan limits, deg	$4 \le 2\theta \le 42$	unique rflns	4956
scan method	Wyckoff	unique rflns with ($F_o \ge 5\sigma(F_o)$)	2964
std rflns	3 std/197 rflns		
R(int)	0.047	GOF	1.77
R_f,[a] %	8.30	highest peak, final diff map, e Å^{-3}	1.99
R_{wf},[a] %	8.00		
Δ/σ (last cycle)	0.02	g[a]	0.001
no. of param ref	219		

[a] $w^{-1} = \sigma^2(F_o) + gF_o^2$; $R_f = \sum|\Delta|/\sum|F_o|$; $R_{wf} = \sum(|\Delta|w)/\sum(|F_o|w)$; $\Delta = |F_o| - |Fc|$.

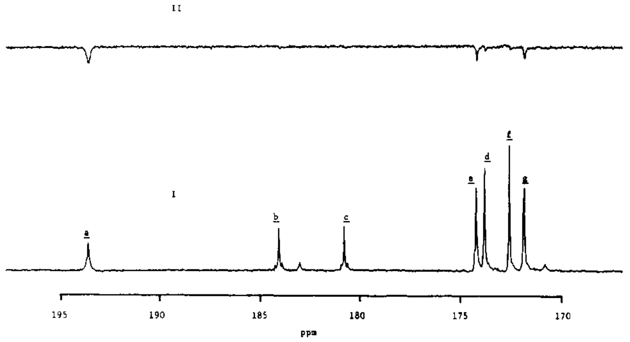

Figure 2. ^{13}C NMR magnetization-transfer experiment for $Os_3(CO)_{11}(\mu\text{-}CH_2)$ (1). (I) ^{13}C NMR spectrum of 1 in $CDCl_3$ showing only the CO region. (II) Difference spectrum obtained after selective saturation of the downfield resonance at δ 193.4.

mation was obtained by using ^{13}C NMR spectroscopy to evaluate the effect on the carbonyl ligands. ^{13}C NMR magnetization-transfer experiments on $Ru_3(CO)_{11}(\mu\text{-}CH_2)$ showed that the μ-CO ligand (a) exchanges with the axial CO (b) on the back Ru atom, and this was the basis for the mechanistic proposal of Scheme I. The results of a similar ^{13}C NMR magnetization transfer experiment for 1 are shown in Figure 2, with the labels corresponding to those in Scheme I. The downfield resonance labeled a is assigned to the bridging CO, and those labeled b and c are attributed to the unique axial CO's on the back Os atom. The other four resonances d, e, f, and g of relative intensity 2 are due to the four remaining pairs of equivalent CO's, but they cannot be individually distinguished. Similar assignments have been made for $Ru_3(CO)_{11}(\mu\text{-}CH_2)^3$ and $[HOs_3(CO)_{11}]^{-11}$ which have similar structures. As shown in Figure 2, selective irradiation of resonance a due to the bridging CO of 1 resulted in a loss of intensity in resonances e and g, *but no loss of intensity in resonances b and c due to the back axial carbonyls was observed.*

The results of the magnetization-transfer experiments clearly show the occurrence of some process which exchanges the methylene hydrogens and some of the carbonyl ligands. However, the results are different from those obtained by Shapley and co-workers for $Ru_3(CO)_{11}(\mu\text{-}CH_2)$ and are not consistent with the mechanism of Scheme I with the methylene ligand of 1 migrating from a bridging to a terminal position. The precise details of the exchange process for $Os_3(CO)_{11}(\mu\text{-}CH_2)$ cannot be defined from the available data, but the results are not inconsistent with the intermediacy in the exchange process of the previously proposed[2a] ketene complex 6. As shown below, if the ketene ligand in 6 were to lie in the Os_3 plane, when it collapses back to 1, exchange of the bridging CO with the equivalent pair of terminal CO's on the front Os atoms would occur. Thus, the previous suggestion of the intermediacy of 6 in the various reactions of 1 is not refuted by the present data, and it may well provide the route for the synthesis of 2.

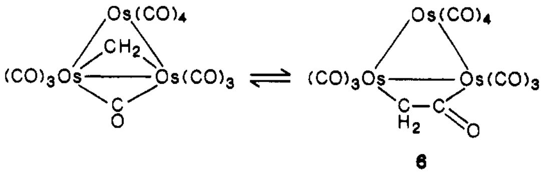

6

Experimental Section

The complexes $Os_3(CO)_{11}(\mu\text{-}CH_2)^{1a}$ and $(Ph_3P)_2Pt(C_2H_4)^{12}$ were prepared by published procedures. Carbon monoxide (CP grade) was obtained from Matheson and used as received. ^{13}CO (90% ^{13}C) was obtained from the Monsanto Research Corp., Mound Laboratories, Columbus, OH. Solvents used were dried and degassed by standard methods. All manipulations, unless otherwise specified, were conducted under prepurified N_2 with use of standard Schlenk and high vacuum line techniques. Infrared spectra were obtained on an IBM FT IR/32 spectrometer with 0.5-mm NaCl solution cells. NMR spectra were recorded on a Bruker WP-200 Fourier transform spectrometer and on a Bruker WH-400 at the NSF Regional NMR Facility in Columbia, SC. Field desorption mass spectra were obtained by Dr. Guy Steinmetz and R. J. Hale at the Tennessee Eastman Co., Kingsport, TN. Elemental analyses were performed by Schwartzkopf Microanalytical Laboratory, Woodside, NY.

Synthesis of $Os_3Pt(\mu\text{-}CH_2)(CO)_{11}(PPh_3)_2$ (2). A THF solution (20 mL) of $(Ph_3P)_2Pt(C_2H_4)$ (72 mg, 0.096 mmol), was added by cannula to a well-stirred solution of $Os_3(CO)_{11}(\mu\text{-}CH_2)$ (85 mg, 0.095 mmol) in 210 mL of THF. The initial red color of the solution faded to light orange after 15 min, and the solvent was removed under high vacuum to give an orange oil which was chromatographed on SiO_2 using CH_2Cl_2/hexane (60:40, v/v) as eluent. One yellow band was isolated which yielded 104 mg of 2 (68% based on 1) as a yellow powder. Recrystallization from Et_2O gave 2 as analytically pure yellow platelets. Anal. Calcd for $C_{48}H_{32}O_{11}Os_3P_2Pt$: C, 35.75; H, 2.00. Found: C, 35.89; H, 2.23. IR (THF): 2103 (w), 2053 (m), 2025 (sh), 2016 (s), 1989 (m), 1975 (w) and 1945 (w) cm^{-1}. Mass spectrum: *m/z* (FD) 1613 (M^+). ^1H NMR (C_6D_6, 22 °C): δ 7.53–7.00 (m, Ph's), 4.50 (d, $J_{H\text{-}P}$ =

---

(11) Eady, C. R.; Johnson, B. F. G.; Lewis, J.; Malatesta, M. C. *J. Chem. Soc., Dalton Trans.* **1978**, 1358–1363.

(12) Blake, D. M.; Roundhill, D. M. *Inorg. Synth.* **1978**, *18*, 120–124.

5.5 Hz, μ-CH_2). ^{31}P NMR (C_6D_6, 22 °C): δ 35.6 (d, J_{P-P} = 9.8 Hz, J_{P-Pt} = 2797 Hz), 25.3 (d, J_{P-Pt} = 4806 Hz). ^{13}C NMR (THF-d_8, 22 °C): δ 76.5 (dt, J_{C-H} = 147 Hz, J_{C-P} = 56 Hz, μ-CH_2).

Reaction of 2 with CO. Carbon monoxide was rapidly bubbled through a THF solution of 2 (34 mg, 0.021 mmol). The yellow solution lightened over the course of 10 min after which time the reaction was judged complete by IR monitoring. Solvent evaporation under high vacuum gave a mixture of $Os_3Pt(\mu$-$CH_2)(CO)_{12}(PPh_3)$ (5) and PPh_3, which gave 2 upon standing. 5: IR (THF) 2110 (w), 2060 (m), 2043 (m), 2024 (s), 1995 (m), 1982 (sh), 1964 (vw), 1958 (vw) cm^{-1}; ^1H NMR (C_6D_6, 22 °C) δ 7.66–6.86 (m, Phs), 4.30 (m, μ-CH_2); ^{31}P NMR (CD_2Cl_2, −80 °C) δ 20.8 (s, J_{P-Pt} = 4088 Hz), −6.6 (s, PPh_3); ^{13}C NMR (THF-d_8, 22 °C) δ 73.1 (t, J_{C-H} = 146 Hz, μ-CH_2).

Reaction of 2 with PhC≡CPh. Diphenylacetylene (54 mg, 0.300 mmol) was added to a THF solution of 2 (25 mg, 0.015 mmol). Monitoring of the reaction solution by IR spectroscopy showed that the ν_{CO} bands due to 2 disappeared over the course of 3 days and were replaced by bands at 2102 (w), 2066 (m), 2045 (m), 2012 (s), 2000 (m), 1973 (m), and 1960 (br, w) cm^{-1}. Solvent evaporation gave a red oil which was chromatographed on SiO_2 (CH_2Cl_2 eluant) to give PhC≡CPh and a trace of 2 as the only bands that eluted.

Magnetization-Transfer Experiments on 1. ^1H NMR (200.13 MHz) magnetization-transfer experiments were performed on a Bruker WP-200 spectrometer. Selective saturation of the downfield resonance (δ 7.75) was achieved with minimum decoupler power, and the intensity of the upfield signal was measured after a variable length delay. The data were then analyzed by literature methods.[11] The ^{13}C NMR saturation-transfer experiment was performed on a Bruker WH-400 spectrometer. Data were obtained by using a DANTE pulse train with the resonance at δ 193.4 due to the μ-CO selectively saturated by setting the transmitter on that peak. The observed spectrum was then subtracted from a previously collected ^{13}C NMR spectrum of 1 to give the difference spectrum shown in Figure 2.

Crystallographic Structure Determination of 2. Crystalline samples of 2 obtained by recrystallization from diethyl ether, occurred as layers (book pages) of yellow, very fine, and poorly aligned flakes. Only a plate of single thickness produced sufficiently narrow line widths to allow collection of satisfactory diffraction data. The best specimen of ten screened had dimensions of 0.04 × 0.32 × 0.36 mm and displayed expected, severe edge effects for reflections with small glancing angles (<3°) (maximum/minimum transmission = 0.68/0.23). An empirical absorption correction routine (XEMP), which attempts to fit a thin plate (major face = 100) to the data, was used; reflections with a glancing angle of ≤3° were discarded resulting in the loss of 395 data. As judged by the behavior of the anisotropic thermal parameters of the lighter atoms and by the values of R(int), other methods for correction of absorption effects, both empirical and analytical, were less satisfactory.

The "E statistics" and $Z = 8$ suggested the centrosymmetric space group alternative $C2/c$, and all processing of data was confined to this choice. The structure was solved by direct methods without difficulty. Due to the low fraction of undiscarded observed data, only the Os, Pt, P, carbonyl group, and methylene bridge atoms were refined anisotropically. The phenyl rings were constrained as rigid, planar hexagons (C–C = 1.395 Å). Following anisotropic refinement, a disordered, full-occupancy molecule of the recrystallization solvent Et_2O was located. Further refinement revealed another reduced occupancy site arbitrarily set at half-occupancy. Hydrogen atoms, except for those associated with the disordered molecules of Et_2O which were neglected, were included as idealized contributions. The highest peaks on the final difference map (0.5–1.22 e Å^{-3}) are all associated with the disordered molecules of diethyl ether.

All data collection and processing software are contained in the P3 and SHELXTL program packages distributed by the Nicolet XRD Corp. Pertinent crystallographic data and atomic positional parameters are listed in Tables II and III. Observed and calculated structure factors, atomic coordinates, complete bond distances and angles, anisotropic temperature factors, and hydrogen atom coordinates are available as supplementary material.

Table III. Atomic Coordinates (×10^4) and Isotropic Thermal Parameters (Å^2 × 10^3) for $Os_3Pt(\mu$-$CH_2)(CO)_{11}(PPh_3)_2$

	x	y	z	U
Os(1)	2228.2 (4)	3364.6 (8)	2769.9 (7)	49 (1)^a
Os(2)	1780.0 (3)	2185.8 (8)	3501.1 (6)	41 (1)^a
Os(3)	2089.8 (3)	1659.5 (8)	2179.2 (6)	43 (1)^a
Pt	1414.6 (3)	2362.9 (7)	4761.6 (6)	38 (1)^a
P(1)	1276 (2)	3379 (5)	5594 (4)	45 (3)^a
P(2)	1086 (2)	1125 (5)	5009 (4)	43 (3)^a
O(1)	1610 (6)	4025 (14)	1886 (11)	79 (10)^a
O(2)	214 (7)	5020 (14)	3672 (12)	102 (13)^a
O(3)	2776 (6)	2732 (14)	3826 (10)	70 (9)^a
O(4)	2720 (7)	3978 (16)	1647 (13)	110 (13)^a
O(5)	2522 (6)	2035 (15)	863 (11)	82 (10)^a
O(6)	2699 (7)	958 (17)	3066 (13)	102 (13)^a
O(7)	1404 (7)	2221 (17)	1466 (11)	105 (12)^a
O(8)	1896 (6)	−257 (14)	1868 (12)	84 (11)^a
O(9)	1411 (6)	418 (14)	3299 (11)	85 (11)^a
O(10)	2337 (6)	1408 (18)	4490 (13)	76 (11)^a
O(11)	1151 (7)	3158 (19)	2888 (14)	121 (14)^a
C(1)	1828 (8)	3765 (18)	2216 (13)	45 (12)^a
C(2)	2223 (10)	4399 (22)	3328 (17)	76 (16)^a
C(3)	2580 (8)	2911 (22)	3398 (18)	69 (14)^a
C(4)	2538 (7)	3749 (18)	2065 (15)	45 (12)^a
C(5)	2356 (8)	1889 (18)	1352 (14)	48 (12)^a
C(6)	2484 (9)	1227 (21)	2754 (17)	71 (11)^a
C(7)	1677 (11)	2005 (19)	1708 (16)	77 (17)^a
C(8)	1961 (8)	458 (19)	2008 (15)	53 (13)^a
C(9)	1576 (9)	1011 (23)	3377 (15)	69 (15)^a
C(10)	2136 (12)	1685 (23)	4123 (19)	83 (20)^a
C(11)	1379 (10)	2803 (19)	3062 (15)	70 (15)^a
C(12)	1748 (8)	3153 (16)	4312 (14)	48 (12)^a
C(21)	665 (6)	3590 (12)	4894 (9)	58 (9)
C(22)	317	3772	4816	94 (13)
C(23)	127	3981	5420	120 (16)
C(24)	284	4006	6102	110 (15)
C(25)	631	3823	6180	73 (11)
C(26)	822	3615	5576	48 (8)
C(31)	1814 (5)	4538 (11)	5554 (9)	43 (8)
C(32)	1979	5328	5402	71 (10)
C(33)	1793	6040	5128	69 (11)
C(34)	1442	5962	5007	91 (13)
C(35)	1277	5173	5160	75 (11)
C(36)	1463	4461	5433	39 (8)
C(41)	1404 (6)	3863 (10)	7004 (11)	67 (10)
C(42)	1502	3738	7724	100 (14)
C(43)	1582	2896	7975	71 (10)
C(44)	1563	2180	7506	88 (12)
C(45)	1465	2305	6786	62 (9)
C(46)	1385	3147	6535	42 (8)
C(51)	617 (5)	1521 (12)	6044 (10)	62 (9)
C(52)	461	1461	6712	69 (10)
C(53)	573	838	7216	110 (15)
C(54)	842	276	7052	110 (15)
C(55)	998	336	6384	64 (10)
C(56)	886	959	5880	58 (9)
C(61)	692 (5)	1514 (11)	3795 (10)	61 (9)
C(62)	404	1427	3348	88 (12)
C(63)	159	791	3498	79 (11)
C(64)	202	242	4095	65 (10)
C(65)	490	328	4543	64 (10)
C(66)	736	964	4393	33 (7)
C(71)	1678 (5)	233 (10)	5151 (9)	38 (8)
C(72)	1901	−478	5091	75 (11)
C(73)	1782	−1280	4821	62 (10)
C(74)	1440	−1372	4611	92 (13)
C(75)	1217	−662	4671	63 (10)
C(76)	1336	140	4941	47 (8)
C(81)	679 (20)	3298 (55)	−1545 (40)	248 (34)
C(82)	579 (20)	2460 (49)	−1185 (44)	223 (31)
C(83)	577 (21)	2458 (50)	570 (49)	247 (35)
C(84)	648 (24)	3112 (59)	1197 (48)	301 (42)
O(12)	601 (16)	2712 (37)	−324 (34)	302 (28)
C(91)	703 (37)	5155 (89)	3141 (72)	205 (57)
C(92)	458 (35)	4374 (82)	2769 (65)	164 (46)
O(13)	114 (37)	4091 (55)	2563 (87)	276 (54)

[a] Equivalent isotropic U defined as one-third of the trace of the orthogonalized U_{ij} tensor.

Organometallics **1986,** *5,* 2233–2243 2233

Acknowledgment. We thank the Department of Energy, Office of Basic Energy Sciences, for support of this research and the donors of the Petroleum Research Fund, administered by the American Chemical Society, for an undergraduate summer research fellowship to C.A.M. Also acknowledged are the National Science Foundation for contributing funds toward the purchase of the diffractometer at the University of Delaware, G. Steinmetz and R. Hale (Tennessee Eastman Co.) for obtaining mass spectra, and A. Freyer (Penn State) for assistance with the ^1H NMR saturation-transfer experiments. The DANTE ^{13}C saturation-transfer experiment was performed at the National Science Foundation Regional Facility in NMR at the University of South Carolina (Grant No. CHE 82-07445). We gratefully acknowledge the assistance of Drs. Alan Benesi and Helga Cohen in obtaining these results.

Registry No. 1, 77208-32-3; 2, 104324-86-9; 5, 104324-87-0; $Pt(PPh_3)_2(CH_2{=}CH_2)$, 12120-15-9; Os, 7440-04-2; Pt, 7440-06-4.

Supplementary Material Available: Tables of anisotropic temperature factors, bond lengths and angles, and hydrogen atom coordinates and a plot of kinetic data from the ^1H NMR magnetization transfer experiment for 2 (5 pages); a list of structure factors (19 pages). Ordering information is given on any current masthead page.

Reactions of $(\mu\text{-}H)_2Rh_2[P(O\text{-}i\text{-}Pr)_3]_4$ with Hydrogen. A Novel Isocyanide Hydrogenation Reaction

Stephen T. McKenna,*† Richard A. Andersen, and Earl L. Muetterties‡

Department of Chemistry, University of California, Berkeley, California 94720

Received November 5, 1985

The reaction of the compounds $(\mu\text{-}H)_2(RNC)Rh_2[P(O\text{-}i\text{-}Pr)_3]_4$ ($R = 4\text{-}ClC_6H_4$, $PhCH_2$) with H_2 yields $(\mu\text{-}H)(\mu\text{-}RNMe)Rh_2[P(O\text{-}i\text{-}Pr)_3]_4$, formally the result of transfer of three hydrogens to the isocyanide carbon and reduction of the triple bond to a single bond. The X-ray crystal structure of $(\mu\text{-}H)(\mu\text{-}4\text{-}ClC_6H_4NMe)Rh_2[P(O\text{-}i\text{-}Pr)_3]_4$ (monoclinic, $P2_1/n$, $a = 13.960$ (2) Å, $b = 19.430$ (2) Å, $c = 21.825$ (2) Å, $\beta = 91.36$ (1)°, $Z = 4$; $R = 0.042$, $R_w = 0.056$ for 5098 data with $I > 3\sigma$) shows two RhP_2 units bridged by the arylmethylamido group and the hydride (not located) with a geometry slightly twisted out of planarity. The intermediate in the reaction, the formimidoyl species $H(\mu\text{-}H)_2(RN{=}CH)Rh_2[P(O\text{-}i\text{-}Pr)_3]_4$, can be detected by multinuclear NMR. Upon further reaction with H_2, low conversions to the secondary amines RNHMe plus $H(\mu\text{-}H)_3Rh_2[P(O\text{-}i\text{-}Pr)_3]_4$ are observed. Reaction of $(\mu\text{-}H)(\mu\text{-}RNMe)Rh_2[P(O\text{-}i\text{-}Pr)_3]_4$ with additional RNC results in a mixture of $(\mu\text{-}H)(\mu\text{-}RNMe)Rh[P(O\text{-}i\text{-}Pr)_3]_3(RNC)$, the result of substitution of a phosphite by RNC, and mononuclear products. For the reaction of $(\mu\text{-}H)_2(RNC)Rh_2[P(O\text{-}i\text{-}Pr)_3]_4$ ($R = n\text{-}Bu$, $t\text{-}Bu$, and $2,6\text{-}Me_2C_6H_3$) with H_2, substitution and fragmentation processes compete with the hydrogenation reaction and little or no $(\mu\text{-}H)(\mu\text{-}RNMe)Rh_2[P(O\text{-}i\text{-}Pr)_3]_4$ is produced. Under D_2, the complexes $(\mu\text{-}H)(\mu\text{-}RNMe)Rh_2[P(O\text{-}i\text{-}Pr)_3]_4$ display H/D exchange via an intramolecular oxidative addition process which results in selective D incorporation into the phosphite methyl positions, as well as the ortho and benzylic positions of the amido ligand in the compound with $R = PhCH_2$.

Introduction

The reduction of C≡O and C≡N triple bonds is a process of extreme practical importance. However, unlike C≡C triple bond hydrogenation, for which homogeneous catalytic processes are well-known,[1-3] useful soluble catalysts for reducing C≡O and C≡N triple bonds are rare. Complexes of the form $HRhP_2$ have been found to catalyze the hydrogenation of nitriles to primary amines under mild conditions;[4] hydridoruthenium phosphine complexes are reported to do the same under more forcing conditions.[5] The clusters $Ni_4(RNC)_7$ catalyze the hydrogenation of isocyanides to secondary amines.[6] Catalytic systems for the hydrogenation of CO to alcohols[7,8] or alkanes[9] have been reported, but conditions are typically severe and the natures of the active species are unclear. In none of these cases are mechanistic details known.

Scheme I

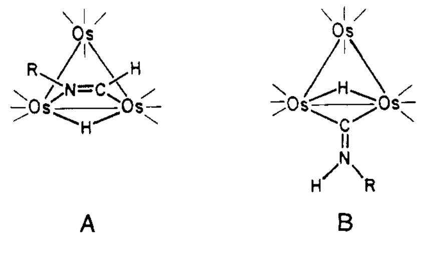

A stoichiometric hydrogenation of CO to bound methoxide has been observed by Bercaw and co-workers.[10] The reaction of $[(C_5Me_5)_2Zr(N_2)]_2(\mu\text{-}N_2)$ with CO followed by H_2 appears to proceed by attack of $(C_5Me_5)_2ZrH_2$ on the proposed intermediate formyl complex $(C_5Me_5)_2Zr(H)(CHO)$ to give $(C_5Me_5)_2Zr(H)(OMe)$. Under slightly different conditions, the unique binuclear enediolate complex

---

† Address correspondence to this author at Amoco Research Center, P.O. Box 400, Naperville, IL 60566.

‡ Deceased January 12, 1984.

(1) (a) Collmann, J. P.; Hegedus, L. *Principles and Applications of Organotransition Metal Chemistry*; University Science Books: Mill Valley, CA, 1980. (b) Parshall, G. W. *Homogeneous Catalysis*; Wiley: New York, 1980.

(2) Muetterties, E. L.; Krause, M. J. *Angew. Chem., Int. Ed. Engl.* **1983**, *22*, 135.

(3) (a) Burch, R. R.; Muetterties, E. L.; Teller, R. G.; Williams, J. M. *J. Am. Chem. Soc.* **1982**, *104*, 4257. (b) Burch, R. R.; Shusterman, A. J.; Muetterties, E. L.; Teller, R. G.; Williams, J. M. *J. Am. Chem. Soc.* **1983**, *105*, 3546.

(4) Yoshida, T.; Okano, T.; Otsuka, S. *J. Chem. Soc., Chem. Comm.* **1979**, 870.

(5) Grey, R. A.; Pez, G. P.; Wallo, A. *J. Am. Chem. Soc.* **1981**, *103*, 7536.

0276-7333/86/2305-2233$01.50/0